Liquid Crystals
Publication details, including instructions for authors and subscription information:
http://www.informaworld.com/smpp/title~content=t713926090

The structure, conformation and orientational order of fluorinated liquid crystals determined from carbon-13 NMR spectroscopy

E. Ciampi

Online publication date: 06 August 2010

To cite this Article Ciampi, E.(1999) 'The structure, conformation and orientational order of fluorinated liquid crystals determined from carbon-13 NMR spectroscopy', Liquid Crystals, 26: 1, 109 — 125
To link to this Article: DOI: 10.1080/026782999205614
URL: http://dx.doi.org/10.1080/026782999205614

LIQUID CRYSTALS, 1999, VOL. 26, NO. 1, 109–125

The structure, conformation and orientational order of fluorinated liquid crystals determined from carbon-13 NMR spectroscopy

E. CIAMPI, M. I. C. FURBY, L. BRENNAN, J. W. EMSLEY*
Department of Chemistry, University of Southampton, Southampton, UK

A. LESAGE and L. EMSLEY
Laboratoire de Stéréochimie et des Interactions Moléculaires,
UMR-117 CNRS/ENS, Ecole Normale Supérieure de Lyon, 46 Allée d'Italie,
69364 Lyon, France

(*Received 6 June 1998; in final form 26 August 1998; accepted 8 September 1998*)

The ^{13}C-$\{^1H\}$ NMR spectra of two monofluorinated nematic liquid crystals, I35 and I52, have been obtained and analysed to yield sets of dipolar couplings, D_{iF}, from each carbon in the molecule to the fluorine nucleus. The couplings involving carbons in the fluorinated biphenyl group are used, together with a mean field theoretical model (the Additive Potential, AP), to determine the shape of the potential governing rotation about the inter-ring bond. For both molecules this is found to have a minimum when the two phenyl rings are at either 40° or 140° to one another. For I35 the couplings involving the aliphatic carbons are used to determine that the minimum energy forms for rotation about the aromatic ring to alkyl chain bonds are when the chains are orthogonal to the rings; the data for I52 are consistent with the same conformations. The AP model predicts that the conformer probabilities for the molecules in the nematic phase are substantially different from those in the isotropic phase at the same temperature.

1. Introduction

The molecules which form liquid crystalline phases are invariably flexible by virtue of internal bond rotational motion. This means that the molecules exist in a range of conformational states, and this affects their orientational order [1]. The reverse is also true, so that the conformational distribution adopted by the molecules is dependent in part on the orientational order. The nature of this conformation–orientation interdependence can be investigated by NMR spectroscopy. This can be achieved by measuring the partially-averaged quadrupolar splittings, $\Delta\nu_i$, from deuteriated samples [2], but this requires the synthesis of deuteriated samples, which can be a difficult task. Proton NMR spectra may yield dipolar couplings, D_{ij}^{HH}, between protons, but this requires the analysis of very complex spectra. The simplification of such spectra to the point where they can be resolved and analysed usually involves partial deuteriation followed by deuterium decoupling, and perhaps also the use of multiple quantum spectroscopy [3]. Again, this is a difficult task. It is demonstrated here that a set of dipolar couplings, D_{ij}^{CF}, between the carbons and the fluorine can be obtained much more easily for liquid crystal molecules which contain a single fluorine atom, such as those of the *Imn* series, and a study of two members, I35 and I52, whose structures are shown in figure 1, is presented here. It is shown that the D_{ij}^{CF} can be used to explore the conformational distributions in these molecules, and to determine how this depends on orientational order.

The experiment is in principle quite simple. The carbon spectrum is recorded whilst decoupling all the interactions to the protons. The result should be a doublet splitting for each non-equivalent carbon nucleus, which yields the dipolar couplings. In practice, however, it has proved difficult to decouple the protons from the carbons when the dipolar couplings are large. Thus, Nanz *et al.* [4] studied I52, primarily as an example of the efficiency of different decoupling schemes, but they did not succeed in obtaining an analysable spectrum. In particular they found that although quite good decoupling could be obtained with their decoupling schemes for the aromatic carbons, the result for the aliphatic carbons was an almost complete failure. A similar result was obtained

*Author for correspondence.

Journal of Liquid Crystals ISSN 0267-8292 print/ISSN 1366-5855 online
http://www.tandf.co.uk/JNLS/lct.htm
http://www.taylorandfrancis.com/JNLS/lct.htm

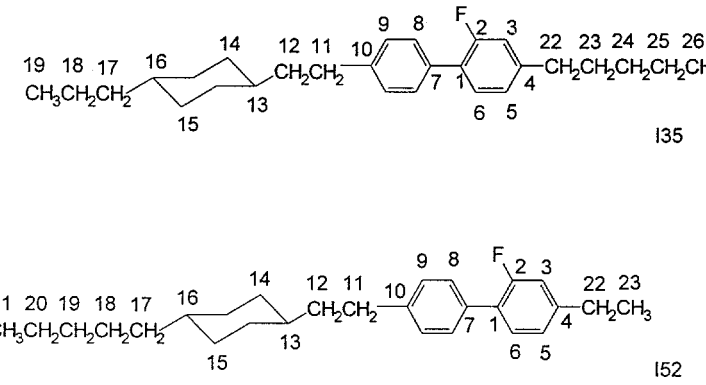

Figure 1. Structures and atomic labelling of I35 and I52.

by Sandstrom and Levitt [5] in a study of the mesogen 4-*n*-pentyl-4′-cyanobiphenyl, 5CB. They were successful in decoupling the aromatic carbons, and were able then to measure inter-carbon dipolar couplings amongst the ring carbons by a 2D double quantum experiment, but again they could not efficiently decouple the aliphatic carbons.

One solution to the problem of decoupling when the dipolar couplings are large is to reduce their magnitudes by rotating the sample at an angle θ to the magnetic field which is close to the magic angle [6]. This a useful way of obtaining the larger D_{ij}^{CF}, but does not reveal the smaller, long range couplings. We show that by recording a series of spectra at different values of θ it is possible to assign the spectrum from a static spectrum, and hence to obtain a complete set of the D_{ij}^{CF} for the two mesogens I52 and I35.

2. Experimental

2.1. *NMR experiments on isotropic samples*

The samples of I35 and I52 were obtained from Merck Ltd, UK. ^{13}C-{^{1}H} spectra on samples dissolved in $CDCl_3$ were obtained at 75 MHz, as shown in figure 2, which yielded the chemical shifts and ^{13}C-^{19}F scalar coupling constants, J_{iF}, shown in table 1. For each sample, the assignment of the carbon resonances of the spectrum from an isotropic solution was based on the following series of experiments. ^{13}C-{^{1}H} DEPT experiments at 75 MHz were used to distinguish between C, CH, CH_2 and CH_3 carbons. The method used to give a detailed assignment of the carbon spectra will be illustrated for I52. The first step was to record a proton spectrum at 500 MHz on $CDCl_3$ solutions, as illustrated in figure 3, and to assign the lines in this spectrum with the aid of a double-quantum-filtered 2D COSY proton spectrum, which is shown in figure 4. A proton-detected HSQC 2D experiment then enabled the carbon resonances to be assigned—see figure 5. These experiments enabled most of the ^{13}C lines to be assigned, but some ambiguities in assignment remained in those cases where either the proton or carbon resonances are not well resolved. The main purpose of obtaining an assignment of the ^{13}C-{^{1}H} of the $CDCl_3$ solution was so as to be able to assign the resonances in the spectrum of the two compounds in their nematic phases. As we shall see, a combination of the information from the spectra of the isotropic and nematic samples is necessary to arrive at an unambiguous assignment of both types of spectra.

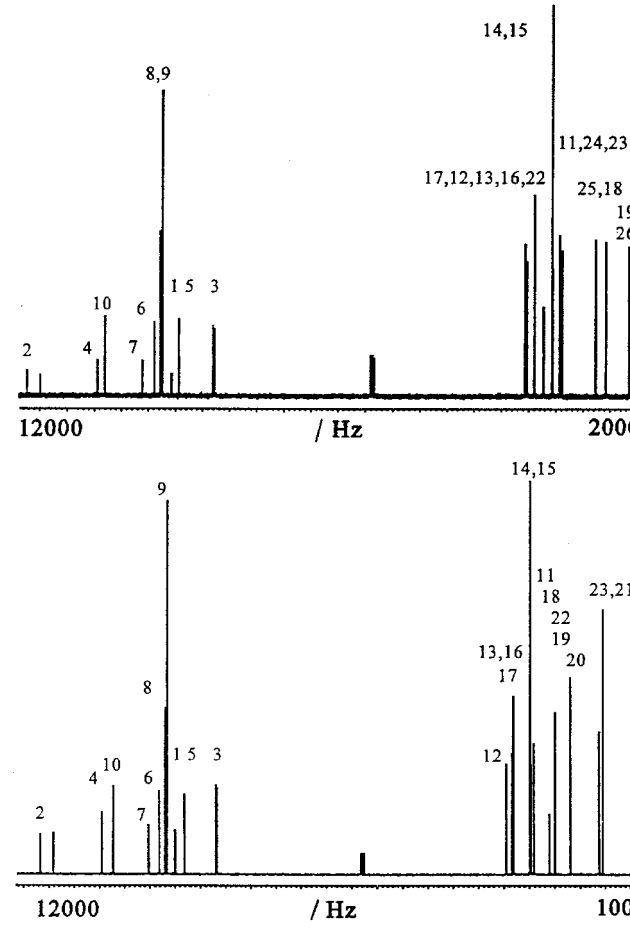

Figure 2. 75 MHz ^{13}C-{^{1}H} spectra of solutions of I35 (top) and I52 (bottom) in $CDCl_3$.

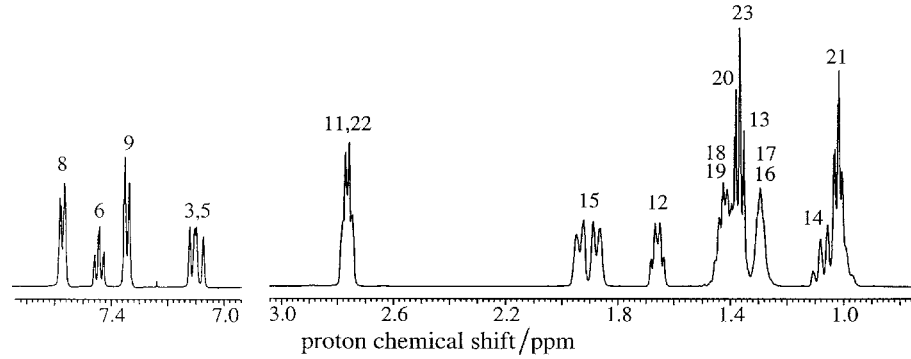

Figure 3. 500 MHz ^{1}H spectrum of a sample of I52 dissolved in $CDCl_3$.

Table 1. Chemical shifts δ_i relative to $CDCl_3$ (at 77.22 ppm) and coupling constants J_{iF} for the carbon atoms in samples of I35 and I52 dissolved in $CDCl_3$.

Carbon atom	I35		I52	
	δ_i/ppm[a]	J_{iF}/Hz[b]	δ_i/ppm[a]	J_{iF}/Hz[b]
1	126.818	13.3	126.383	13.1
2	160.371	− 247.3	159.972	− 247.3
3	116.320	22.3	115.371	22.1
4	144.903	7.6	145.340	7.3
5	124.988	3.1	123.934	2.5
6	130.930	4.2	130.524	3.3
7	133.826	1.1	133.324	0.0
8	129.464	2.8	128.921	2.6
9	129.059		128.550	
10	143.145		142.591	
11	33.784		32.492	
12	40.509		39.573	
13	38.250		37.746	
14	33.990		33.492	
15	33.960		33.492	
16	38.248		38.083	
17	40.037		37.625	
18	20.751		32.317	
19	15.131		26.970	
20			22.994	
21			14.374	
22	36.087		28.513	
23	31.549		15.393	
24	32.155			
25	23.233			
26	14.719			

[a] ±0.003 ppm.
[b] ±0.5 Hz.

2.2. ^{13}C-{^{1}H} experiments on static, nematic samples

The first task to be addressed in order to obtain good ^{13}C-{^{1}H} spectra from the nematic samples was how to achieve good proton decoupling. Nanz *et al.* [4] have recently applied a number of decoupling schemes to a sample of I52. They found that multiple pulse schemes gave the best results, but they did not succeed in obtaining a spectrum with well resolved lines which could be analysed to yield the ^{13}C-^{19}F spin–spin couplings. Their experiments were performed on a high resolution spectrometer with limited decoupling power. Their decoupling field is quoted as being 21 kHz, corresponding to a 90° pulse of approximately 10 μs. They used an acquisition time of 0.1 s, and accumulated 256 decays. They do not quote a delay between acquisitions, which in fact is crucial for obtaining good resolution when decoupling liquid crystalline samples. The delay allows heat to be lost, and prevents a rise in temperature. There is therefore an optimum combination of acquisition time, decoupler power and delay time in order to achieve good decoupling without broadening the lines because of sample heating. In our ^{13}C experiments at 50.3 MHz these parameters were a 5 μs 90° proton pulse at 200 MHz, acquisition in 0.1 s, and a 10 s delay time. The transmitter carrier frequency of the proton irradiation must also be carefully optimized.

The ^{13}C experiments were done on a Bruker MSL 200 spectrometer using a high power, double-tuned, single coil solenoid probe. The sample was approximately 10 mm long and was contained in a 5 mm o.d. tube, mounted horizontally; a teflon vortex plug was used to prevent the liquid flowing out of the tube. The sample temperature was maintained at 305 K. Both I35 and I52 have melting points close to room temperature, and are both rather viscous at this temperature, which is probably giving rise to a natural linewidth greater than the probe resolution. We found it expedient to reduce the viscosity by adding a solute. Two solutes were tried. The first was hexamethyldisiloxane, HMDSO, which has the advantage of giving a peak in the carbon spectrum at higher field than those in the liquid crystals, and of having a high boiling point so that the samples could be raised above their nematic–isotropic temperatures in order to adjust the magnet homogeneity. In later experiments we also used benzene as a solute. This has the disadvantage of giving a peak in the aromatic region of the spectrum, but has the advantage that the homogeneity of the magnetic field could be optimized by

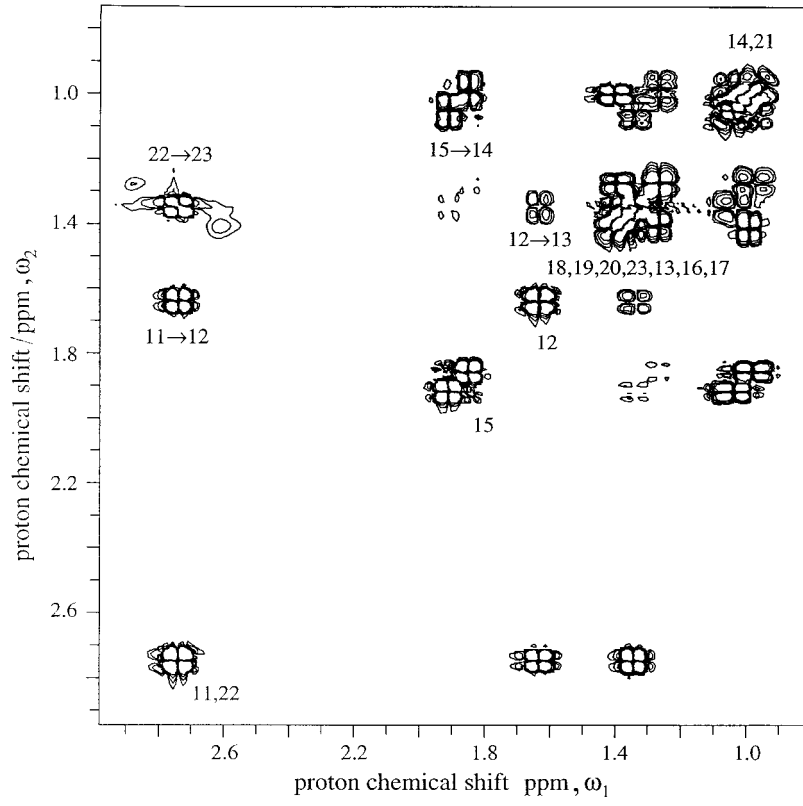

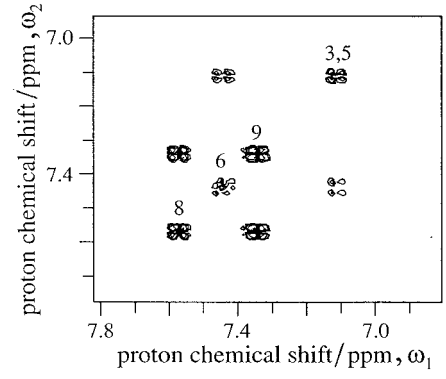

Figure 4. 500 MHz ^{1}H DQF-COSY spectrum of a sample of I52 dissolved in $CDCl_3$.

observing the sharp lines from the proton spectrum at the same temperature used to record the carbon spectra.

We repeated the experiments of Nanz *et al.* [4] on both I52 and I35, and in agreement with them found the best results for sequences COMARO-2, which was very similar to WALTZ-16. Table 2 gives the details of the pulse sequences used in these experiments. The spectrum obtained for I35 using COMARO-2 is shown in figure 6. This is in fact better resolved in the aromatic region and has better line intensities than that obtained by Nanz *et al.* on I52, but like them we found that good decoupling of the aliphatic carbons could not be achieved. The assignment of the lines given in figure 6 will be discussed later.

Table 2. The proton decoupling pulse sequences COMARO-2 and Sandström-Levitt (SL).

COMARO-2
$(385°y\ 320°\text{-}y\ 25°y\ 385°x\ 320°\text{-}x\ 25°x)_3\ (385°\text{-}y\ 320°y\ 25°\text{-}y\ 385°x\ 320°\text{-}x\ 25°x)_3$
Sandström-Levitt
$(Dx\ Dy\ D\text{-}x\ D\text{-}y)$ where $D = 1.5$ ms.

Figure 6 also shows the spectrum obtained by a decoupling scheme, SL, introduced by Sandstrom and Levitt [5] to obtain ^{13}C-^{13}C dipolar couplings by the 2D double quantum experiment. Sandstrom and Levitt

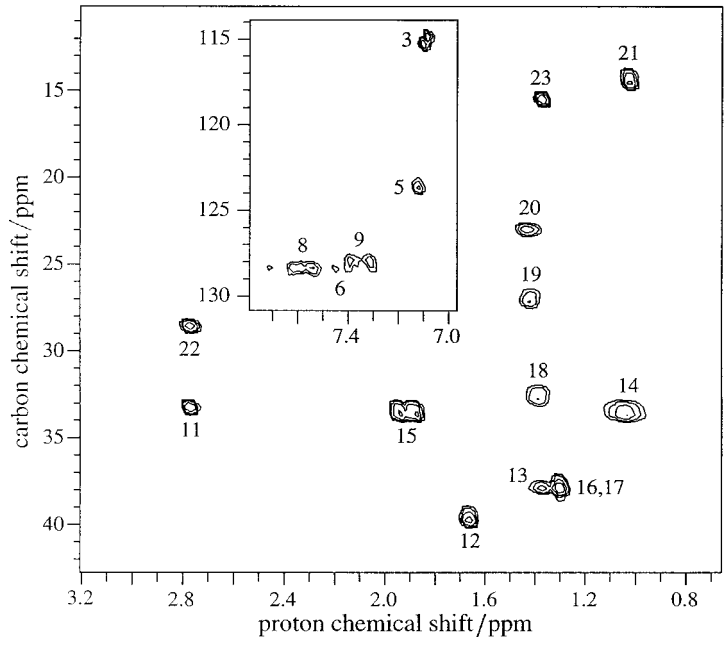

Figure 5. 500 MHz HSQC ^{1}H-^{13}C correlation spectrum of a sample of I52 dissolved in $CDCl_3$.

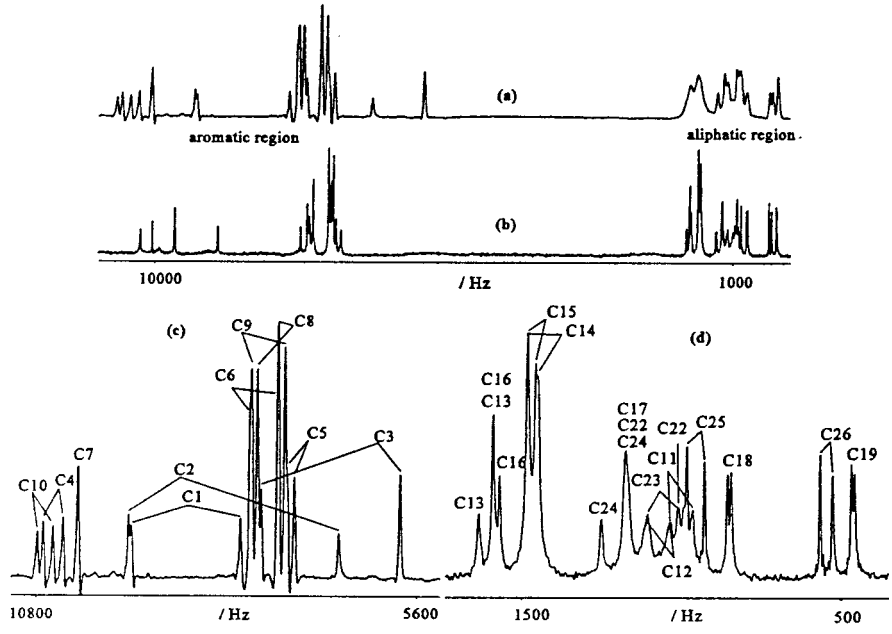

Figure 6. 50.3 MHz ^{13}C-{^{1}H} spectra of static samples of I35 at 310 K in the nematic phase of I35 containing (*a*) 10% HMDSO and (*b*) 10% benzene. The spectra were obtained with (*a*) COMARO-2 and (*b*) SL decoupling. Expansions of the aromatic region in (*a*) is shown in (*c*), and an expansion of the aliphatic region of (*b*) is shown in (*d*).

state that good decoupling of the aromatic carbons could be achieved, but not of the aliphatic carbons in their experiments on the nematogen 5CB. We find that for 5CB very good decoupling of all the carbons can be achieved with the SL sequence, but only by a careful adjustment of the proton centre frequency, O2. For I35 and I52 careful adjustment of O2 also leads to good decoupling of the aliphatic carbons, as shown in figure 6. The aromatic region at first sight also seems very well decoupled, but closer examination reveals that some lines in the spectrum are missing, and are probably broadened beyond detection. These lines are from carbons 1, 2, and 3, which are those with the largest couplings to the fluorine.

2.3. *VASS spectra on nematic samples*

The assignment of the static spectra was achieved by obtaining a series of spectra in which the sample is rotating about an axis making an angle θ with the magnetic field [6]. When a nematic liquid crystalline sample with a positive anisotropy $\Delta\chi$ in the magnetic susceptibility (which is the case for the *Imn*) is rotated

above a threshold frequency, the director aligns along the spinning axis if $0° < \theta < 54.7°$. The anisotropic interactions are all reduced from their static values by a factor

$$R(\theta) = (3\cos^2\theta - 1)/2 \quad (1)$$

so that at the magic angle the spectrum should be identical to that of an isotropic sample. As θ is decreased from this angle, the anisotropic contributions, δ_i^{aniso} to the chemical shift δ_i, and D_{ij} to the spin–spin coupling, $T_{ij} = J_{ij} + 2D_{ij}$, increase in magnitude. Thus,

$$\delta_i(\theta) = \delta_i^0 + R(\theta)\delta_i^{\text{aniso}} \quad (2)$$

$$T_{ij}(\theta) = J_{ij} + R(\theta)2D_{ij}. \quad (3)$$

^{13}C-{^{1}H} VASS spectra were acquired for both I35 and I52 with a Bruker probe type MAS 200 SB BL7. The samples were contained in glass bottles which fit snugly into the 7 mm rotor. The probe has a single, double tuned solenoid coil and spectra cannot be obtained in this probe for $\theta < 43°$. The proton decoupling power for the VASS probe corresponds to a 90° pulse duration of 7 μs.

Figure 7 shows VASS spectra obtained for I35 containing HMDSO for the aromatic region, using CAMARO-2 decoupling, whilst figure 8 shows the spectra on the same sample for the aliphatic carbons using SL decoupling. The angle is set by a micrometer control, calibrated by recording deuterium spectra of a sample of benzene-d_6 dissolved in I35. The doublet for C2 in figure 7 at first decreases as θ increases from 54°, passes through zero, and then increases steadily. This is because J_{2F} and D_{2F} are of opposite sign, and since J_{2F} is expected to be negative, this determines D_{2F} to be positive. The relative signs of the scalar and dipolar couplings involving carbons 1 and 3 with the fluorine can also be obtained by comparing the doublet splittings on these carbon resonances for $\theta = 53°$ with the J_{iF} values obtained for the isotropic solution. This gives the relative signs shown in table 3. The D_{ij} values within the rigid, fluorinated aromatic fragment are given by

$$D_{ij} = -(K_{ij}/r_{ij}^3)[S_{zz}^{\text{R}}(3\cos^2\theta_{ijz} - 1) + (S_{xx}^{\text{R}} - S_{yy}^{\text{R}})(\cos^2\theta_{ijx} - \cos^2\theta_{ij}) + 4S_{xz}^{\text{R}}\cos\theta_{ijx}\cos\theta_{ijz}] \quad (4)$$

with

$$K_{ij} = (\mu_0/4\pi)\hbar\gamma_i\gamma_j/8\pi^2.$$

The angles θ_{ijx} etc. are between the x axis and $\mathbf{r}_{ij}$, the inter-nuclear vector. The xyz axes are fixed in the ring, as shown in table 4, and S_{xx}^{R} etc. are local order parameters for these axes. As we shall see later, the signs of the D_{iF} can be established, and therefore this enables the absolute signs of the J_{iF} to be obtained.

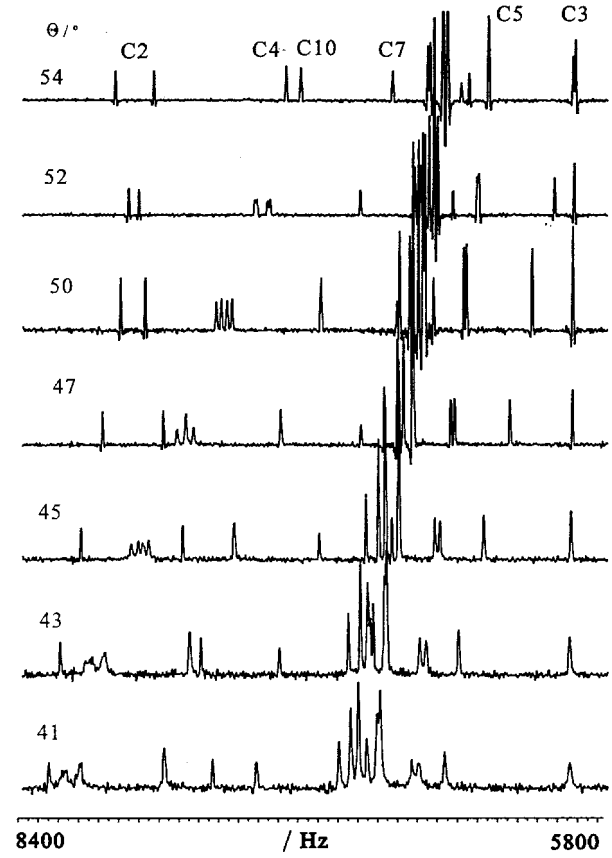

Figure 7. 50.3 MHz ^{13}C-{^{1}H} VASS spectra of the aromatic carbons of a sample of I35 in the nematic phase containing 10% HMDSO. The angles θ of the rotation axis with respect to the magnetic field are shown against each spectrum. The COMARO-2 sequence was used for decoupling; this produces the best resolution for the aromatic carbons.

The spectrum corresponding to $\theta = 54.7°$ is very similar, as expected, to that obtained for the solution in chloroform, and so the assignments of the lines in these two spectra are the same. The chemical shifts of each carbon can then be followed up to the spectrum with $\theta = 43°$, and this is illustrated for the aromatic and aliphatic carbons of I35 in figures 9 and 10 where the shifts are plotted against the reduction factor $R(\theta)$. Fitting a straight line to these plots gave the slopes as δ_i^{aniso}, which are listed in table 3, and enables a value for $\theta = 0°$ to be obtained by extrapolation; the same procedure produced the values of δ_i^{aniso} for I52, which are also given in table 3. The splittings resolved in each of the VASS spectra can be used to obtain $D_{ij}(\theta)$, and plotting these against $R(\theta)$ produces estimates for the D_{ij} of a stationary sample.

Note that for each liquid crystal four different sets of spectra were recorded: (1) VASS spectra, and (2) a spectrum on a stationary sample, in each case with decoupling by the COMARO-2 sequence, to produce

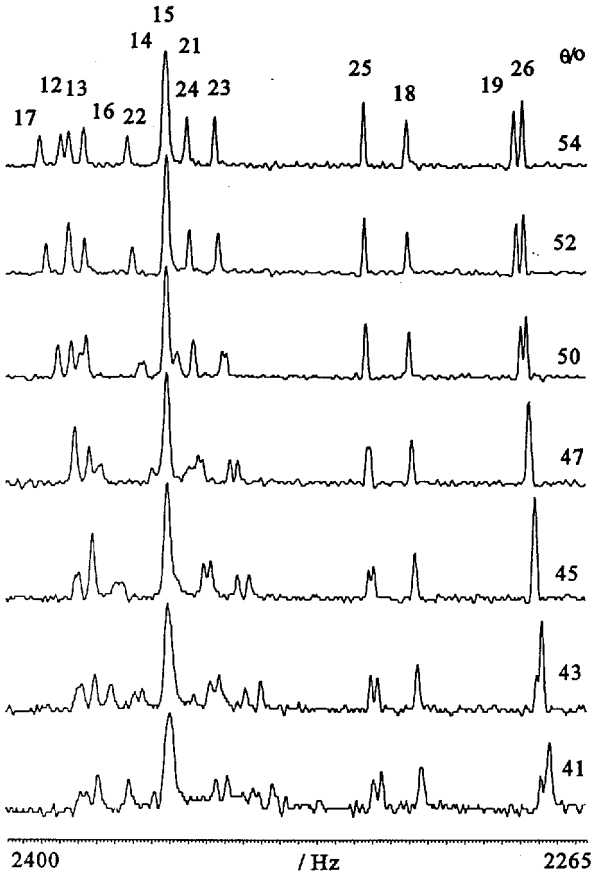

Figure 8. 50.3 MHz ^{13}C-{^{1}H} VASS spectra of the aliphatic carbons of a sample of I35 in the nematic phase containing 10% benzene. The angles θ of the rotation axis with respect to the magnetic field are shown against each spectrum. The SL sequence was used for decoupling; this produces the best resolution for the aliphatic carbons.

the data on the aromatic carbons; (3) VASS spectra, and (4) a spectrum on a stationary sample, in each case with decoupling by the SL sequence, to give data for the aliphatic carbons. The spectra of the stationary samples were recorded on a different probe from the VASS spectra, at nominally the same, but probably a slightly different temperature, and so exact agreement between these spectra and those simulated using the extrapolated shifts and coupling constants is not expected. For each liquid crystal, and separately for the aromatic and aliphatic regions, the spectrum simulated with parameters produced by an extrapolation of the data obtained in the VASS experiments was then used as the starting point for an iterative fitting of the observed and calculated spectral envelopes by the program WINFIT (Bruker). This produced a set of dipolar couplings and chemical shifts for the aromatic region of the spectrum of the static sample containing 10% HMDSO, and a similar set for the aliphatic region, but these two data sets were not obtained under identical conditions of decoupling, and those couplings which were well resolved in both spectra differed in magnitude by a few percent. This difference most probably arises because of a different heating effect of the two decoupling methods used. To correct for the different recording conditions it was necessary to scale the $D_{i\mathrm{F}}$ values for the aliphatic carbons derived from the spectra obtained by SL decoupling. The scaling factor was determined by comparing those $D_{i\mathrm{F}}$ which were well resolved in the spectra obtained by the two decoupling methods. The $D_{i\mathrm{F}}$ obtained in this way for all the carbons in each mesogen are given in table 3. Note the large uncertainties on $D_{11\mathrm{F}}$ for both I35, and I52. These are because the lines from these carbons were never fully resolved in either the VASS or static spectra.

3. Relating the $D_{i\mathrm{F}}$ to the structure, conformation and orientational order of the molecules

The anisotropic spin–spin coupling between a pair of nuclei, neither of which is a proton, may have a contribution from the anisotropic part, J_{ij}^{aniso}, of the nucleus–electron–electron–nucleus coupling mechanism. This pseudo-dipolar coupling appears in the spin hamiltonian in the same form as the direct, through space contribution, which is normally referred to as the dipolar coupling, D_{ij}, so that the two interactions cannot be obtained separately from an NMR spectrum. The dipolar couplings depend simply on the magnitude and orientation of the inter-nuclear vector, but this is not the case for J_{ij}^{aniso}, which has a complex dependence on electronic structure. It is reasonable to assume that J_{ij}^{aniso} will be finite only if the isotropic J_{ij} is non-zero, and so in the present case we need consider only the possible importance of this term for couplings in the aromatic rings. A detailed study of fluorobenzene [7] dissolved in a nematic solvent concluded that $J_{\mathrm{CF}}^{\mathrm{aniso}}$ is negligibly small, and this will be assumed to be the case for I35 and I52.

3.1. *The rigid fragment containing the fluorine atom*

In the fragment

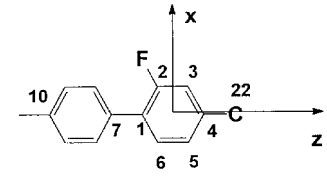

in both I35 and I52, the dipolar couplings to the numbered carbon atoms should obey equation (4), and they have been used to obtain the local order parameters. To do this the structure shown in figure 11 was adopted for these fragments; this uses bond lengths and angles obtained from a geometry-optimized *ab initio* molecular orbital calculation [8]. Note that $D_{11\mathrm{F}}$ in I35 and I52

Table 3. The dipolar couplings D_{iF} and the chemical shift anisotropies δ_i^{aniso} for the carbons in I35 and I52 when a static sample containing 10% HMDSO is in the nematic phase. The signs in parentheses are assigned to be in agreement with the predictions of the calculations with the AP model.

Carbon atom	I35		I52	
	D_{iF}/Hz	δ_i^{aniso}/Hz	D_{iF}/Hz	δ_i^{aniso}/Hz
1	705.4 ± 2.0	2361.8 ± 15.2	666.1 ± 2.0	2312.1 ± 9.8
2	1502.1 ± 2.0	54.8 ± 5.7	1381.9 ± 2.0	65.1 ± 3.1
3	− 922.7 ± 2.0	1002.0 ± 6.7	− 888.4 ± 2.0	1004.5 ± 6.6
4	− 135.8 ± 2.0	3167.5 ± 29.2	− 131.4 ± 2.0	3137.1 ± 17.1
5	45.4 ± 2.0	1089.2 ± 8.0	41.6 ± 2.0	1105.1 ± 6.6
6	179.9 ± 15.0	1152.5 ± 6.7	183.1 ± 2.0	1141.8 ± 12.6
7	0.0 ± 10.0	3414.3 ± 22.1	0.0 ± 10.0	3309.8 ± 19.7
8	− 216.5 ± 15.0	1167.1 ± 8.5	− 205.4 ± 2.0	1142.0 ± 12.3
9	− 139.9 ± 2.0	1197.5 ± 7.5	− 126.8 ± 2.0	1118.5 ± 7.8
10	− 105.1 ± 2.0	3351.6 ± 30.4	− 102.0 ± 2.0	3293.0 ± 15.3
11	(−)42 ± 20.0	− 595 ± 32	(−)25 ± 5.0	− 706 ± 17
12	(−)38.5 ± 5.0	− 832 ± 12	(−)53 ± 5.0	− 846 ± 19
13	(−)26 ± 2.0	− 136 ± 3	(−)27 ± 2.0	− 106 ± 3
14	(−)21.5 ± 2.0	− 33 ± 2	(−)23 ± 2.0	− 28 ± 1
15	(−)13.5 ± 2.0	− 33 ± 2	(−)15 ± 2.0	− 28 ± 1
16	(−)12.5 ± 2.0	− 128 ± 3	(−)12 ± 2.0	− 120 ± 3
17	(−)1 ± 10.0	− 766 ± 7	(−)10 ± 3.0	− 792 ± 13
18	(−)7 ± 2.0	− 132 ± 2	(−)6 ± 2.0	− 423 ± 6
19	(−)7 ± 2.0	− 132 ± 2	(−)6 ± 2.0	− 423 ± 6
19	(−)6 ± 2.0	− 306 ± 4	(−)10 ± 3.0	− 363 ± 7
20			(−)2.5 ± 2.0	− 155 ± 4
21			(−)4.5 ± 2.0	− 222 ± 5
22	(−)102 ± 5.0	− 574 ± 35	(−)104 ± 4.0	− 614 ± 12
23	(−)73.5 ± 2.0	− 419 ± 4	(−)82 ± 2.0	− 71 ± 2
24	(−)51.5 ± 2.0	− 304 ± 4		
25	(−)33.5 ± 2.0	− 122 ± 2		
26	(−)23 ± 2.0	− 158 ± 5		

was not well determined and was not included in these calculations, although it is part of the rigid fragments. Varying only the three order parameters to bring the calculated D_{iF} into closest agreement with those observed gave good but not perfect agreement. The agreement was then improved by allowing the position of the fluorine atom to vary by rotation about C2 with a constant bond length of $r_{CF} = 1.35$ Å. The change in the bond angle C1C2F was found to be 0.8° for both I35 and I52. The order parameters obtained are shown in table 4. The new position for the F atom was kept fixed for all subsequent calculations. Note that the differences, ΔD_{iF} between observed and calculated dipolar couplings are all acceptably small except ΔD_{6F}. This large error probably arises because the peaks from this carbon are not well resolved in the spectra, and so D_{6F} is not obtained with high precision. We have therefore not used this dipolar coupling in subsequent calculations.

3.2. *The effect of bond rotational motion on the dipolar couplings*

The bond notational motion in these molecules is fast enough to average the dipolar couplings between nuclei in different rigid groups. The averaged couplings are given by [1]

$$D_{ij} = \int D_{ij}(\beta, \gamma, \phi_i) P_{LC}(\beta, \gamma, \phi_i) \sin\beta \, d\beta \, d\gamma \, d\phi_i \quad (6)$$

where $D_{ij}(\beta, \gamma, \phi_i)$ is the dipolar coupling when the director is at an orientation in the molecular reference frame given by the polar angles β and γ, whilst in a conformation specified by a set of bond rotational angles ϕ_i. $P_{LC}(\beta, \gamma, \phi_i)$ is the probability that a molecule is at this orientation and in this conformation. In order to calculate the averaged D_{ij} from equation (5) it is necessary to choose a model for $P_{LC}(\beta, \gamma, \phi_i)$, and we have used the Additive Potential (AP) model [2]. This expresses $P_{LC}(\beta, \gamma, \phi_i)$ as

$$P_{LC}(\beta, \gamma, \phi_i) = Z^{-1} \exp[-U(\beta, \gamma, \phi_i)/kT] \quad (6)$$

with

$$Z = \int \exp[-U(\beta, \gamma, \phi_i) kT] \sin\beta \, d\beta \, d\gamma \, d\phi_i. \quad (7)$$

Table 4. Optimized geometry of the rigid fragment using D_{iF}^{CF} obtained from the analysis of the ^{13}C-{^{1}H} NMR spectra of I35/HMDSO and I52/HMDSO.

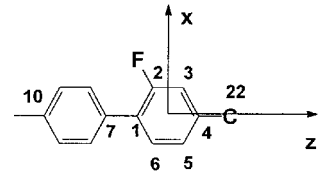

Order parameter	I35	I52
S_{zz}	0.682 ± 0.001	0.653 ± 0.001
S_{xx}-S_{yy}	0.011 ± 0.001	0.018 ± 0.001
S_{xz}	-0.013 ± 0.001	-0.010 ± 0.001

	I35		I52	
i	x/Å	z/Å	x/Å	z/Å
1	0.0	0.746	0.0	0.746
2	−1.171	1.490	−1.171	1.490
3	−1.186	2.867	−1.186	2.867
4	−0.015	3.553	−0.015	3.553
5	1.209	2.850	1.209	2.850
6	1.193	1.467	1.193	1.467
7	0.0	−0.746	0.0	−0.746
10	0.0	−3.540	0.0	−3.540
11	0.0	−5.083	0.0	−5.083
22	0.017	5.070	0.0165	5.070
F	-2.370 ± 0.001	0.87 ± 0.001	-2.370 ± 0.001	0.87 ± 0.001
i	$\Delta D_{iF} = D_{iF}$(calc-obs)	Weight	$\Delta D_{iF} = D_{iF}$(calc-obs)	Weight
1	0.1	1	0.9	1
2	0.1	1	0.1	1
3	0.1	1	0.1	1
4	0.2	1	−0.5	1
5	−1.1	1	−1.0	1
6	7.9	0	−4.0	1
7	1.7	0	−0.3	1
10	−0.3	1	1.4	1
11	−18.0	0	−4.2	1
22	−4.1	1	1.8	1

$U(\beta, \gamma, \phi_i)$ is a conformationally-dependent mean potential, which is divided into a part, $U_{ext}(\beta, \gamma, \phi_i)$, which depends on orientation and conformation (and which vanishes in the isotropic phase) and $U_{int}(\phi_i)$, which depends only on the conformation. The potential of mean torque is expressed as

$$U_{ext}(\beta, \gamma, \phi_i) = -\varepsilon_{2,0}(\phi_i)C_{2,0}(\beta, \gamma) - 2\varepsilon_{2,2}(\phi_i)C_{2,2}(\beta, \gamma). \quad (8)$$

The conformationally-dependent interaction parameters, $\varepsilon_{2,m}(\phi_i)$, are then related to contributions, $\varepsilon_{2,m}(j)$, for each rigid molecular fragment in the molecule by

$$\varepsilon_{2,m}(\phi_i) = \sum_p D^2_{p,m}(\Omega_{ji})\varepsilon_{2,p}(j) \quad (9)$$

where the conformational dependence resides in the Wigner functions, $D^2_{p,m}(\Omega_{ji})$ which describe the orientation of the jth fragment to the molecular reference axis when the molecule is in the ith conformation.

3.3. *The conformational model*

Ideally, the integral in equation (5) should be sampled at small angular intervals for each bond rotation, and

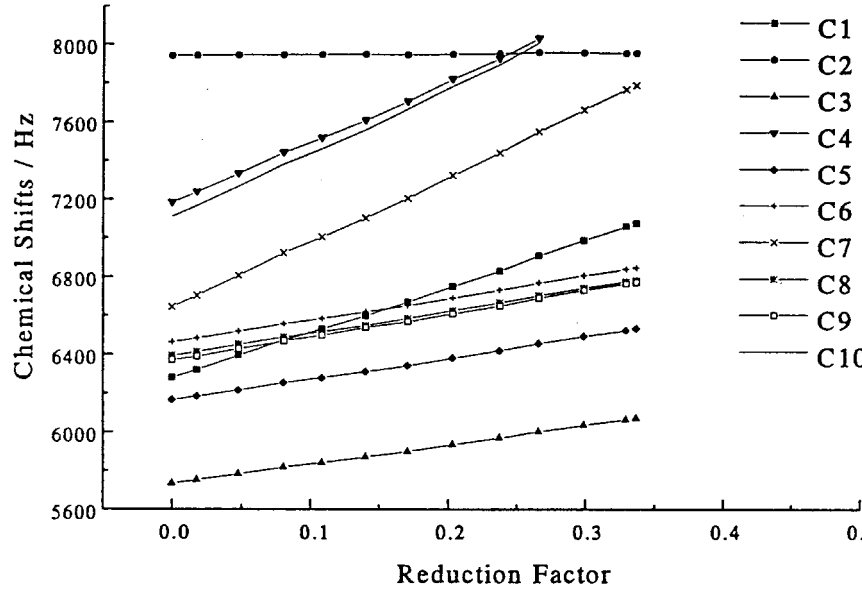

Figure 9. Chemical shifts of the aromatic carbons in a sample of I35 containing 10% HMDSO as a function of the reduction factor, $R(\theta)$, produced by rotating the sample at an angle θ to the magnetic field.

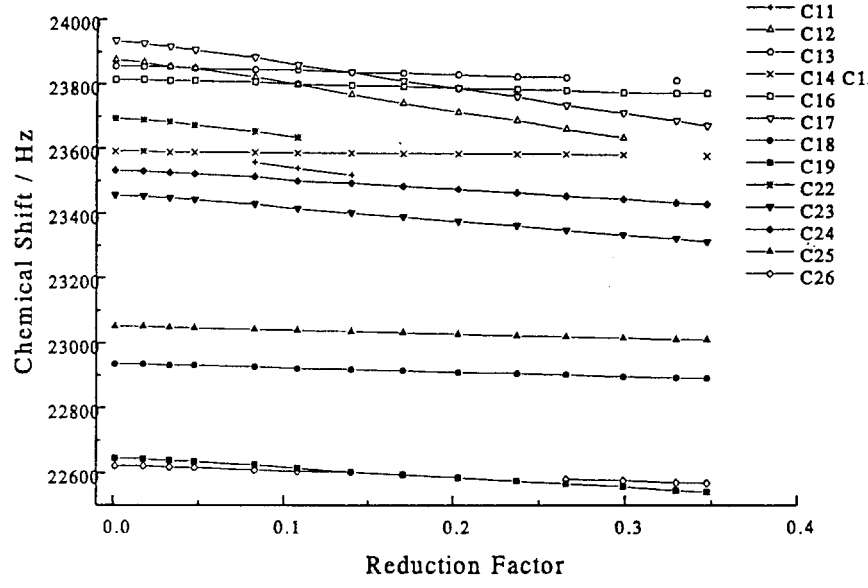

Figure 10. Chemical shifts of the aliphatic carbons in I35 containing 10% benzene as a function of the reduction factor, $R(\theta)$, produced by rotating the sample at an angle θ to the magnetic field.

the calculated D_{iF} brought into agreement with those observed by varying the form of the bond rotational potentials. This is not practicable, nor is it justified by the size of the data set. It is practicable to do such an averaging for the inter-ring bond in the biphenyl group when this is considered as a 4-*R*-4′-*R*′-biphenyl, but when the whole molecules are considered major assumptions have to be made about the conformational distribution. It is then assumed that the molecule moves between a set of minimum energy structures, and the complete set of D_{iF} are used to determine the distribution amongst these conformations, and of how this is affected by the orientational order.

3.4. *Rotation about the inter-ring bond in the biphenyl group*

The rotational potential about the inter-ring bond is investigated by considering the fragment

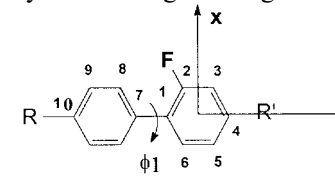

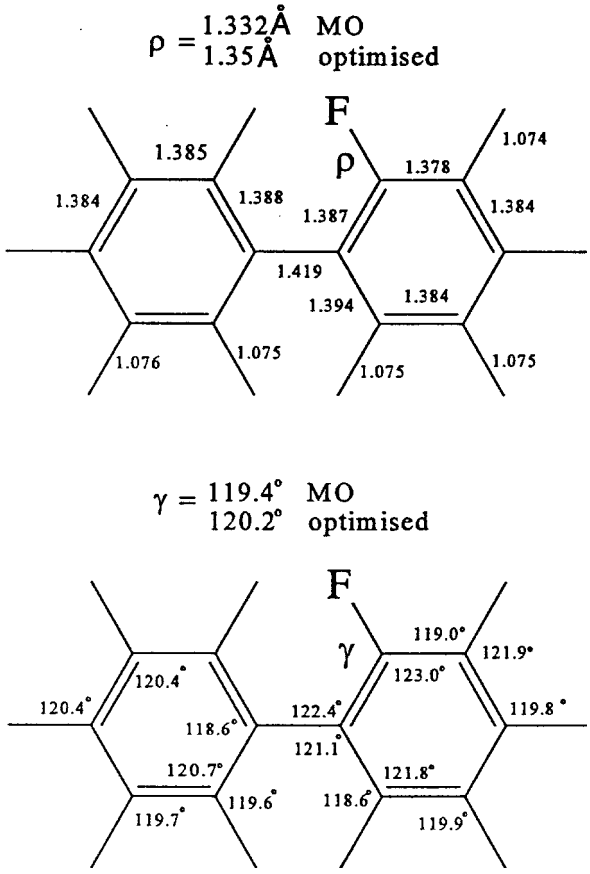

Figure 11. Bond lengths and angles for biphenyl fragments.

where R and R' represent the rest of the molecule. The rigid fragments contributing to equation (9) are

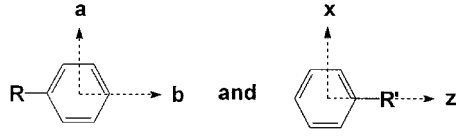

The axes abc (c perpendicular to a and b) and xyz (y perpendicular to x and z) are assumed to be principal axes for the interaction tensors, so that the only non-zero values are ε_{aa}, $\varepsilon_{bb}-\varepsilon_{cc}$, ε_{zz}, and $\varepsilon_{xx}-\varepsilon_{yy}$. The axes a and z are parallel for all values of ϕ_1, and so only the sum $\varepsilon_{aa}+\varepsilon_{zz}$ need be considered, or equivalently we use $\varepsilon_{aa}=\varepsilon_{zz}$. It was also found that the data cannot distinguish separate values of $\varepsilon_{bb}-\varepsilon_{cc}$ and $\varepsilon_{xx}-\varepsilon_{yy}$, and so these too were equated. The remaining fragment is the C–F bond, which has axial symmetry and requires just ε^{CF} directed along the bond. Note that these interaction parameters depend on the nature of R and R'.

The internal potential, $U_{int}(\phi_1)\equiv V(\phi_1)$ was expressed as

$$V(\phi_1)=V_2\cos 2\phi_1+V_4\cos 4\phi_1+U_{steric} \qquad (10)$$

where

$$U_{steric}=\sum_{i,j}E_{ij}[(A_{ij}/r_{ij})^{12}-(A_{ij}/r_{ij})^{6}]. \qquad (11)$$

The summation is over only those pairs of atoms whose distances depend on ϕ_1. The A_{ij} and E_{ij} are constructed from values A_i and E_i [9, 10]:

$$A_{ij}=A_i+A_j \qquad (12)$$

$$E_{ij}=(E_iE_j)^{1/2}. \qquad (13)$$

A_i and E_i depend only on the type of atom, and they were fixed at the values in table 5.

The calculated D_{iF} were brought into best least squares agreement with those observed by varying ε_{zz}, $\varepsilon_{xx}-\varepsilon_{yy}$ and ε^{CF}. Varying both V_2 and V_4 in addition, when the steric term was omitted from equation (10), did not lead to stable iterations, and so V_4 was varied for different, fixed values of V_2. Good agreement was obtained when $V_2=-2.5$ kJ mol^{-1}, as shown in tables 6 and 7. Note that this produces $V(0°)<V(90°)$, which seems unrealistic since the planar structure is strongly sterically hindered. The reason for these relative values of the barrier heights is that when the steric term is absent from $V(\phi_1)$ the minimum energy is when $\phi_1(\min)=1/2\cos^{-1}(-V_2/4V_4)$. If $\phi_1(\min)<45°$, then $V(0°)<V(90°)$, and when $\phi_1(\min)>45°$ then $V(0°)>V(90°)$. When the steric term is included in $V(\phi_1)$ the correlation between $V(0°)$, $V(90°)$ and $\phi_1(\min)$ is removed. It was then possible to vary V_2 and V_4, with the results shown in tables 6 and 7.

The probabilities $P_{LC}(\phi_1)$, which are virtually identical with $P_{iso}(\phi_1)$, are shown in figures 12 and 13. Note that when the steric term is included $V(0°)>V(90°)$, that is $P_{LC}(0°)<P_{LC}(90°)$. For both molecules the effect of including the steric term in $V(\phi_1)$ is to change $\phi_1(\min)$ from 42° to 37°. These angles can be compared with that determined by X-ray diffraction on crystalline 2-fluorobiphenyl [11] (54° ± 3°), and a value of 49° calculated by an *ab initio* molecular orbital calculation on the same molecule [8]. NMR studies on nematic liquid crystalline samples of 4-*n*-pentyl-4′-cyanobiphenyl (5CB) [12] determined $\phi_1(\min)$ to be 38°, whilst a study of a sample of biphenyl [13] dissolved in nematic solvents obtained $\phi_1(\min)=37°$. In both cases the AP method was used, and a steric term was not included in

Table 5. Values of the Lennard–Jones parameters A_i and E_i used in the contribution U_{steric} for rotation about the inter-ring bond through angle ϕ_1 in I35 and I52.

i	A_i/Å	E_i/kJ mol^{-1}
H	2.42	0.03
C	3.55	0.07
F	2.94	0.06

Table 6. Results of bringing observed and calculated D_{ij}^{CF} within the biphenyl group for I35 into agreement by varying ε_{zz}^{R}, $\varepsilon_{xx}^{R} - \varepsilon_{yy}^{R}$, ε_{aa}^{CF}, V_2 and V_4.

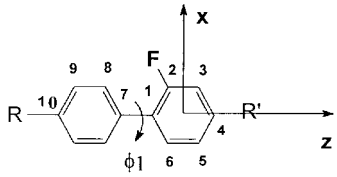

		$\Delta D_{iF} = D_{iF}$(calc)-D_{iF}(obs)/Hz	
i	D_{iF}(obs)/Hz	Without U_{steric}	Including U_{steric}
1	705.4	− 0.8	− 1.1
2	1502.1	0.3	0.3
3	− 922.7	− 0.9	− 1.1
4	− 135.8	0.1	0.1
5	45.5	− 1.2	− 1.2
6	179.9	8.8	8.8
7	—	0.9	0.5
8	− 216.5	− 0.5	− 0.2
9	− 139.9	2.9	2.8
10	− 105.1	− 0.4	− 0.5
V_2/kJ mol^{-1}		− 2.5[a]	− 11.2 ± 2.0
V_4/kJ mol^{-1}		5.5 ± 0.3	0.731 ± 1.7
ε_{zz}^{R}/kJ mol^{-1}		4.58 ± 0.03	4.58 ± 0.02
$\varepsilon_{xx}^{R} - \varepsilon_{yy}^{R}$/kJ mol^{-1}		1.2 ± 0.2	1.2 ± 0.2
ε_{aa}^{CF}/kJ mol^{-1}		− 0.34 ± 0.02	− 0.34 ± 0.02
ϕ_1 (min)/°		42 ± 1	37 ± 1

[a] Fixed.

Table 7. Results of bringing observed and calculated D_{ij}^{CF} within the biphenyl group for I52 into agreement by varying ε_{zz}^{R}, $\varepsilon_{xx}^{R} - \varepsilon_{yy}^{R}$, ε_{aa}^{CF}, V_2 and V_4.

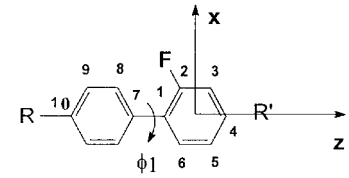

		$\Delta D_{iF} = D_{iF}$(calc)-D_{iF}(obs)/Hz	
i	D_{iF}(obs)/Hz	Without U_{steric}	Including U_{steric}
1	66.1	1.1	0.9
2	1381.9	− 0.1	0.1
3	− 888.4	0.4	0.1
4	− 131.4	− 0.4	− 0.5
5	41.6	− 1.0	− 1.0
6	181.0	− 0.4	− 4.0
7	0.0	0.1	− 0.3
8	− 205.4	0.6	0.9
9	− 126.8	− 3.3	− 2.9
10	− 102.0	1.5	1.4
V_2/kJ mol^{-1}		− 2.5[a]	− 11.0 ± 1.0
V_4/kJ mol^{-1}		5.9 ± 0.4	− 1.49 ± 0.8
ε_{zz}^{R}/kJ mol^{-1}		4.20 ± 0.02	4.20 ± 0.02
$\varepsilon_{xx}^{R} - \varepsilon_{yy}^{R}$/kJ mol^{-1}		0.73 ± 0.08	0.75 ± 0.08
ε_{aa}^{CF}/kJ mol^{-1}		− 0.27 ± 0.02	− 0.27 ± 0.01
ϕ_1 (min)/°		42 ± 1	37 ± 1

[a] Fixed.

the bond rotational potential. An analysis of the data for biphenyl by the maximum entropy method [13], which does not assume a particular form of the bond rotational potential, obtained 34° for ϕ_1(min). It can be concluded that the effect of the F atom in I35 and I52 is to increase ϕ_1(min) by about 4°.

3.5. *The conformation of the alkyl chain attached to the fluorinated ring*

There is evidence that the barrier to rotation about the bond

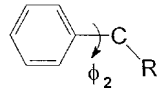

depends on the length of the chain R. Thus, the rotational potential in ethylbenzene has been investigated by microwave spectroscopy and by molecular orbital calculations [14] with the result that it may be approximated as

$$V(\phi_2) = V_2 \cos 2\phi_2 \qquad (14)$$

and has a minimum when $\phi_2 = 90°$ or 270°, that is when the C–R bond is perpendicular to the ring plane. This corresponds to V_2 being positive. The barrier height is only 3 kJ mol^{-1} so that all values of ϕ_2 have an appreciable population at ambient temperature. An NMR study [15] of 5CB in the nematic phase found that V_2 is positive, but the barrier height has increased to >20 kJ mol^{-1}, which means that the C–R bond is essentially confined to being at 90° or 270°. For both I35 and I52 the coupling D_{23F} is sensitive to this rotational potential, but it also depends on the interaction parameter ε^{CC} for the C–C bonds in the alkyl chain. This means that it is not possible to determine the nature of this bond rotational potential in isolation from the motion of the rest of the chain in the case of I35, and of the whole molecule in the case of I52.

For I35 the values of D_{23F}, D_{24F}, D_{25F}, and D_{26F} in the fragment

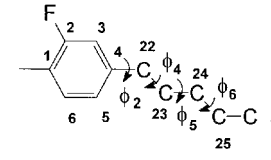

are averaged by motion about the C4–C22 bond. This is assumed to be a jump motion between either two orthogonal forms ($\phi_2 = 90°$ and 270°), or two planar forms ($\phi_2 = 0°$ and 180°). Note that a different value for the angle C4–C22–C23 was used for these two cases:

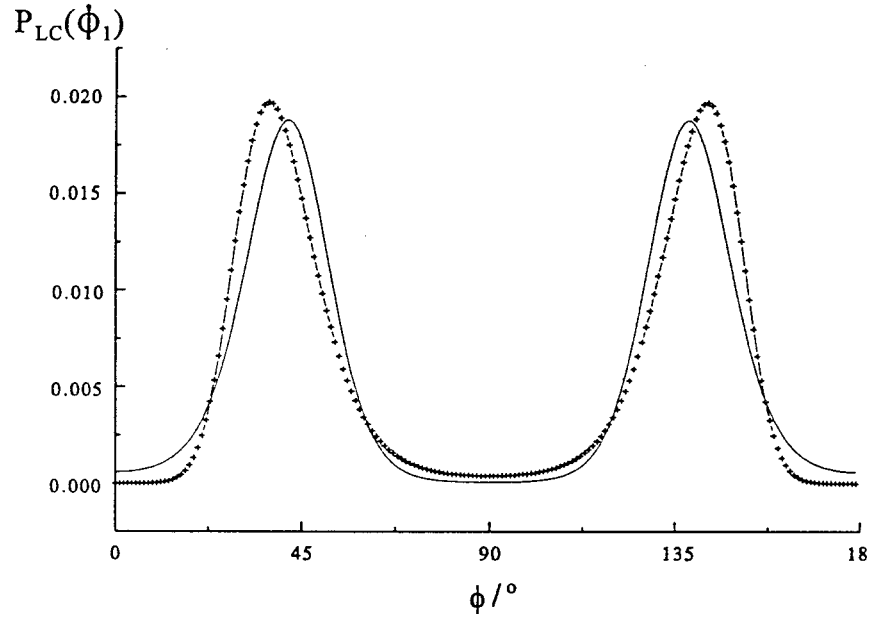

Figure 12. The probability distribution $P_{LC}(\phi_1)$ for rotation about the inter-ring bond in the aromatic part of I35: (– – – –) without and (+ + + +) with the steric term in the rotational potential.

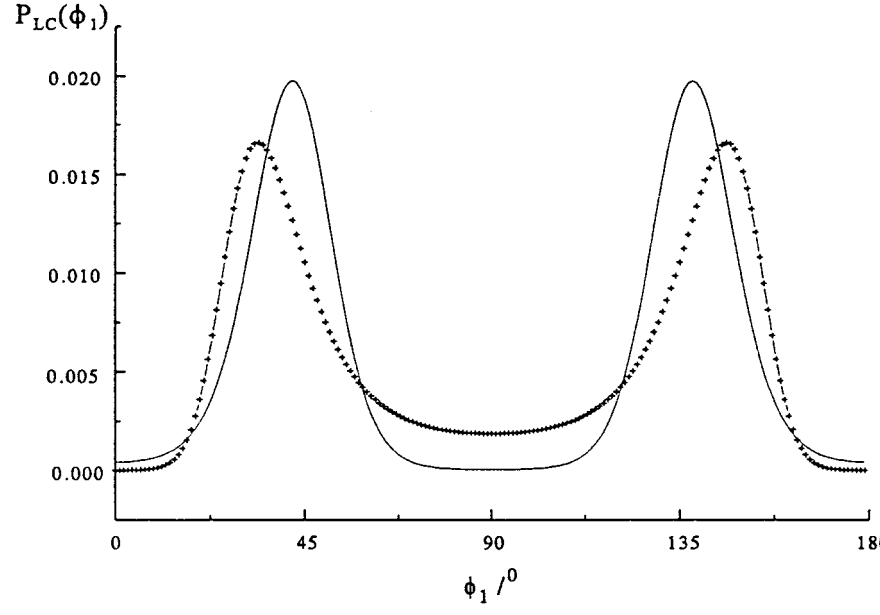

Figure 13. The probability distribution $P_{LC}(\phi_1)$ for rotation about the inter-ring bond in the aromatic part of I52: (– – – –) without and (+ + + +) with the steric term in the rotational potential.

113° for the orthogonal and 120° for the planar forms, based on the molecular orbital calculations of Caminati *et al.* [14]. The couplings to carbons 24–26 are also affected by motion about the C–C bonds through the angles ϕ_4, ϕ_5, and ϕ_6. These rotations are approximated as being jumps between *trans* ($\phi_i = 0°$) and the $\pm$*gauche* forms ($\phi_i = \pm 112°$).

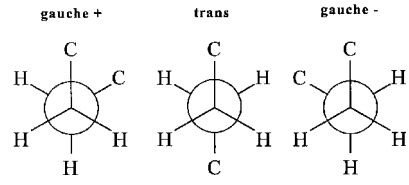

X and Y are the rest of the molecule at either end of the particular C–C bond. The energy difference between the two *gauche* and the *trans* form, E_{tg} was set at 3.4 kJ mol^{-1}, which is close to that used for modelling the chain motion in some alkyl- and alkyloxy-cyanobiphenyl mesogens by the AP method [16].

The ε values to be used for this fragment include ε_{zz}, $\varepsilon_{xx} - \varepsilon_{yy}$ and ε^{CF} for the fluorinated ring, but note that they will not have the same values as those obtained when the aromatic rings and the C–F bond were considered as part of a 4-*R*-4′-*R*′-biphenyl, because of the different contributions in each case from the rest of the molecule. The C–C bonds are assigned a single, equal

value of ε^{CC}. Varying ε_{zz}, $\varepsilon_{xx}-\varepsilon_{yy}$, ε^{CF} and ε^{CC} for the two jump models for motion about C4–C22 gave a good fit to the data only with the chain orthogonal to the ring. The fit improves when an oscillatory motion about the C4–C22 bond through 30° on either side of 90° and 270° is allowed, subject to a potential with $V_2 = 10\,\mathrm{kJ\,mol^{-1}}$, and sampled at intervals of 10°. It is concluded that ϕ_2^{max}, the most probable values for this angle, for I35 are 90° and 270°.

The procedure used to decide between the two models for the ring–chain conformation for I35 cannot be used for I52, since for this molecule the same fragment yields only one coupling, D_{23F}, which depends on this potential. The form of this potential can be investigated only by considering the conformation of the whole molecule.

3.6. *The conformations adopted by the whole molecules*

For the whole molecules the end chains are treated in an identical way. That is, a jump motion about the C–C bonds in the end chains, and about the C11–C12 bond, with an identical value of $E_{tg} = 3.4\,\mathrm{kJ\,mol^{-1}}$, and an equal value of ε^{CC}. The barrier about the bonds linking the cyclohexyl unit to the alkyl chains is assumed to be three-fold in character [17], but with the *gauche* forms having a lower energy than the *trans*. In the absence of an experimental determination of this energy difference, it was assigned the same value of $3.4\,\mathrm{kJ\,mol^{-1}}$ used for the alkyl chain links.

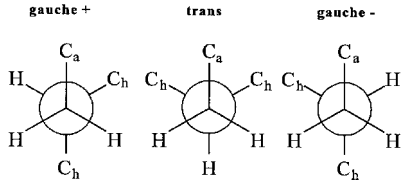

The C_h and C_a are carbon atoms in the cyclohexyl ring and carbon chain respectively. The C–C bonds in the cyclohexyl ring each contribute ε^{CC} to the total interaction tensor.

For both I35 and I52 it was impractical with the computer resources available to allow conformational freedom about all the bonds. Consequently, the conformations about angles ϕ_6 and ϕ_{10} in I35 were restricted to being just the *trans* form, and a similar restriction for ϕ_{12} in I52.

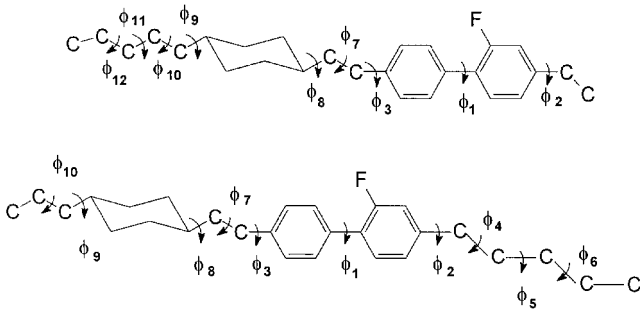

Motion about the biphenyl inter-ring bond was assumed to be jumps between $\phi_1 = 40°$ and 140°; motion through ϕ_2 and ϕ_3 was jumps between 90° and 270°. The complete set of calculated couplings, excluding D_{11F}, for I35, were brought into best agreement with those observed by varying ε_{zz}, $\varepsilon_{xx}-\varepsilon_{yy}$, ε^{CF}, and ε^{CC}. This gave a good fit to the data, and the optimized parameters are shown in table 8. The effect of changing the conformational preference about the C10–C11 bond was explored for I35 by changing the motion to being jumps between values of ϕ_3 of 0° and 180°. This led to substantially worse agreement and can be rejected. Allowing all the ε values to vary for I52, and assuming that ϕ_2 and ϕ_3 are restricted to 90° and 270°, gave a good fit to the data,

Table 8. Results of bringing observed and calculated D_{ij}^{CF} for the whole molecule in I35 and I52 into agreement by varying ε_{zz}^{R}, $e_{xx}^{R}-\varepsilon_{yy}^{R}$, ε_{aa}^{CF} and ε_{aa}^{CC}. The bond rotational motions were jumps between the minimum energy structures, except that motion involving the angles ϕ_6 and ϕ_{10} in I35, and ϕ_{12} for I52 was not allowed and the conformations about these bonds were restricted to being the *trans* form.

	I35	I52
$\varepsilon_{zz}^{R}/\mathrm{kJ\,mol^{-1}}$	2.82 ± 0.02	1.87 ± 0.02
$\varepsilon_{xx}^{R}-\varepsilon_{yy}^{R}/\mathrm{kJ\,mol^{-1}}$	3.49 ± 0.12	9.95 ± 0.12
$\varepsilon_{aa}^{CF}/\mathrm{kJ\,mol^{-1}}$	− 0.30 ± 0.02	− 0.04 ± 0.02
$\varepsilon_{aa}^{CC}/\mathrm{kJ\,mol^{-1}}$	1.42 ± 0.05	1.42 (fixed)

	I35		I52	
i	D_{iF}/Hz	ΔD_{iF}/Hz	D_{iF}/Hz	ΔD_{iF}/Hz
1	705.4	− 0.7	666.1	1.1
2	1502.1	− 0.3	1381.9	− 0.0
3	− 922.7	0.3	− 888.4	0.6
4	− 135.8	0.2	− 131.4	− 0.5
5	45.5	− 1.1	41.6	− 1.1
6	179.9	not used	181.0	− 4.0
7	0.0	not used	0.0	2.2
8	− 21.5	− 0.1	− 205.4	− 0.6
9	− 139.9	2.4	− 126.8	− 4.0
10	− 105.1	− 0.2	− 102.0	1.8
11	− 42	not used	− 25	not used
12	− 38.5	− 7.4	− 53	9
13	− 26	− 2	− 27	0.0
14	− 21.5	− 1.6	− 23	1
15	− 13.5	− 1.8	− 15	0.0
16	− 12.5	− 1.0	− 12	− 1
17	0.0	− 9	− 10	1
18	− 7	− 1	− 6	− 1
19	− 6	0.4	− 10	4
20			− 2.5	− 2
21			− 4.5	1
22	− 102	− 4	− 104	2
23	− 73.5	− 1.9	− 82	not used
24	− 51.5	3.6		
25	− 33.5	0.5		
26	− 23	2		

but gave very different values for the interaction parameters from those obtained for I35. This is contrary to the idea behind the AP method that the fragment contributions for similar molecules with similar ordering should be close in value. The reason for this discrepancy is a combination of the assumption that ϕ_2 is restricted to just 90° and 270°, and that ε^{CC} is identical for all C–C bonds in the molecule. The effect of these two assumptions on the calculated value of D_{23F} cannot be separated. It is probable that the barrier to rotation about C4–C22 in I52 is similar to that in ethylbenzene, that is about 3 kJ mol^{-1}, so that a wide range of values of ϕ_2 are populated, whereas the same barrier in I35 is close to that in 5CB, that is high enough to justify restricting ϕ_2 to just two values. It was decided, therefore, to exclude D_{23F} from the data set for I52, and to fix ε^{CC} at 1.42 kJ mol^{-1}, the value found for I35. Varying the remaining ε values to fit the reduced data set gave the results in table 8.

3.7. *The interdependence of the conformational distribution and the orientational order*

The simplified conformational model still has 972 conformations, and it is impracticable to present the total conformational distribution in detail here. We will confine our discussion to the most striking features of the conformational distributions. In tables 9 and 10 we give the probabilities, $P_{LC}(\phi_i)$ and $P_{iso}(\phi_i)$ of some of the conformations of I35 and I52. The orientational order matrix elements for the representative conformers are also given in tables 9 and 10. They are expressed in the molecular axes xyz, which are fixed in each case in the fluorinated ring. These are not principal axes for the order matrix, and so there are five, independent, non-zero elements in each case.

The 16 most populated conformers have the same probability, 0.0144, in the isotropic phase at the same temperature, and correspond to each CCCC fragment in the alkyl chain portions of the molecules being in the

Table 9. Selected conformations of I35 and their probabilities and orientational order parameters. The conformers are labelled according to their probabilities. In all conformers the value of ϕ_1 is 40°, and ϕ_6 and ϕ_{10} are 0°.

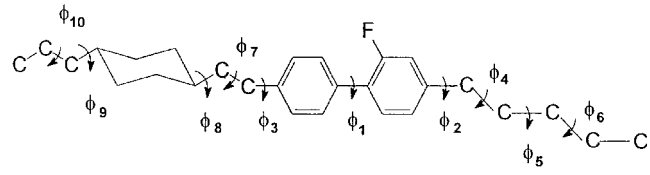

No.	ϕ_2	ϕ_3	ϕ_4	ϕ_5	ϕ_7	ϕ_8	ϕ_9	S_{zz}	S_{xx}-S_{yy}	S_{xy}	S_{xz}	S_{yz}	P_{LC}	P_{iso}
1	90	270	0	0	0	67	293	0.734	−0.056	0.019	−0.077	−0.212	0.028	0.014
16	90	90	0	0	0	67	293	0.763	−0.026	0.007	0.050	−0.013	0.023	0.014
17	270	90	0	0	0	180	67	0.741	−0.013	−0.028	−0.043	0.180	0.007	0.004
19	90	270	0	112	0	293	67	0.743	0.044	0.020	−0.160	−0.109	0.007	0.004
64	90	90	0	0	0	67	180	0.760	−0.014	−0.003	−0.009	−0.051	0.005	0.004
65	90	270	−112	0	0	293	67	0.567	0.046	0.076	−0.118	−0.184	0.002	0.004
71	270	90	0	0	−112	67	67	0.471	0.090	−0.075	−0.137	0.278	0.002	0.004

Table 10. Selected conformations of I52 and their probabilities and orientational order parameters. The conformers are labelled according to their probabilities. In all conformers the value of ϕ_1 is 40°, and ϕ_{11} and ϕ_{12} are 0°.

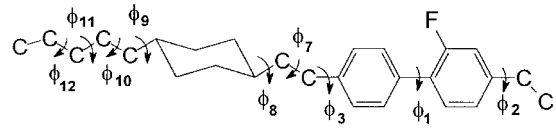

No.	ϕ_2	ϕ_3	ϕ_7	ϕ_8	ϕ_9	ϕ_{10}	ϕ_{11}	S_{zz}	S_{xx}-S_{yy}	S_{xy}	S_{xz}	S_{yz}	P_{LC}	P_{iso}
1	90	270	0	67	293	0	0	0.711	−0.051	0.033	−0.101	−0.217	0.027	0.014
16	90	90	0	67	293	0	0	0.733	−0.029	0.024	0.081	0.121	0.023	0.014
17	270	90	0	180	67	0	0	0.718	0.014	−0.039	−0.077	0.174	0.007	0.004
23	90	270	0	293	67	0	−112	0.740	0.028	0.015	−0.060	−0.122	0.006	0.004
65	90	270	0	293	67	−112	0	0.539	0.112	0.055	−0.099	−0.189	0.002	0.004
69	270	90	−112	67	67	0	0	0.300	0.278	−0.031	−0.230	0.235	0.002	0.004

trans state, whilst the ring chain conformations are also in their minimum energy forms. The degeneracy of these 16 conformations is lifted by the dependence of the contribution to the mean potential from the anisotropic potential of mean torque, $U_{ext}(\beta, \gamma, \phi)$. This term increases in importance with respect to $U_{int}(\phi)$ as the orientational order increases, and is large for both I35 and I52 because the molecules are strongly ordered. The least probable of this set of 16 conformers has the chains at either end of the biphenyl group on the same side of the attached phenyl ring, and similarly the chains attached to the cyclohexyl ring are closest in space, although it is not the spatial proximity of the chains which is disfavouring this conformation, but rather the shape of the molecule is unfavourable when in the nematic field of its neighbours. $P_{LC}(\phi_i)$ for conformer 16 is approximately 20% less than that of conformer 1 for both I35 and I52.

There is a large difference between $P_{LC}(\phi_i)$ and $P_{iso}(\phi_i)$ for each of these 16 conformers. This is also a consequence of the strong orientational order of the molecules. The ratio $P_{LC}(\phi_i)/P_{iso}(\phi_i)$ is ≈ 2 for the most probable conformer, which is reasonable for such well ordered molecules. However, this enhancement in $P_{LC}(\phi_i)$ is dependent on the model used to predict the conformational dependence of the potential of mean torque, and it is also strongly dependent on the assumption that ε^{CC} is the same for all the aliphatic C–C bonds.

The next set of conformers, which have the same values of $P_{iso}(\phi_i)$ of 0.0036, but differ in $P_{LC}(\phi_i)$, have either a *trans* link at one end of the cyclohexyl ring (positions 8 or 9, and a value of 180° for the bond rotation angle), for example conformer 17 in I35 or I52, or a single *gauche* link in the five-membered chain (position 5 for I35, for example conformer 23, and 11 for I52, such as conformer 19, and a value of $\pm 112°$ for the bond rotation angle). In both molecules the single *gauche* link means that the chain is in a 'kink' conformation. For all these conformers, the ratio $P_{LC}(\phi_i)/P_{iso}(\phi_i)$ is similar to that of the top 16 conformers, and they are also well ordered. This is a reflection of their extended shape. Introducing a single *gauche* link at position 4 (conformer 65) or 7 (conformer 71) for I35, and 7 (conformer 65) or 10 (conformer 69) for I52, now leads to an unfavourable shape in the nematic phase and the ratio $P_{LC}(\phi_i)/P_{iso}(\phi_i)$ is ≈ 0.5. The orientational order is also substantially reduced, particularly so for conformer 71 of I35 and 69 of I52.

4. Conclusions

The main conclusion to be drawn from this study is firstly that it is possible to obtain almost all the dipolar couplings between the carbons and a single fluorine in a mesogen by combining the results from VASS spectra to analyse the ^{13}C spectrum of a static sample. To do this it was also necessary to optimize the proton decoupling sequences used, and to apply different sequences to obtain well decoupled aromatic as opposed to aliphatic carbons.

Secondly, it was possible to determine the shape of the rotational potential about the inter-ring bond in the biphenyl group and to locate the minimum in this potential to be at $40° \pm 2°$. This is less than the values of 49° obtained by a geometry-optimized molecular orbital calculation on 2-fluorobiphenyl [8], and 54° determined by an X-ray study on the same molecule in the solid, crystalline form [11].

Thirdly, the conformational preferences about the two aromatic ring–alkyl chain bonds is found to be such that the minimum energy in both cases is when the chain is orthogonal to the attached ring plane, in agreement with the result obtained for the same bond in 4-*n*-pentyl-4′-cyanobiphenyl.

Fourthly, the Additive Potential analysis of the data gives $P_{LC}(\phi_i)$, the conformational distribution for the molecules in the liquid crystalline phase, and $P_{iso}(\phi_i)$, which refers to an isolated molecule in an isotropic environment. These differ because of the contribution to the effective conformational energy of the anisotropic intermolecular potential. Conformers with the most elongated shapes, and hence the most anisotropic, are enhanced in population in the liquid crystalline phase, whilst those with more bent shapes are disfavoured. The effect is large in these molecules because of the large changes in the length to breadth ratios which occur on introducing *gauche* links in the alkyl chains or *trans* at the alkyl chain–cyclohexane link. It is also large because at the temperature of the experiments, which is approximately 60°C below the transition to the isotropic phase, the molecules have a high degree of orientational order.

We wish to acknowledge the award of a studentship to M.I.C.F., and a grant to enable the purchase of the VAS probe, both from the EPSRC. We also wish to thank Mrs Joan Street for recording the ^{13}C spectra on the isotropic samples.

References

[1] Emsley, J. W., 1996, in *Encyclopedia of NMR*, edited by D. M. Grant and R. K. Harris (Chichester: John Wiley & Sons Ltd), p. 2781.

[2] Emsley, J. W., Luckhurst, G. R., and Stockley, C. P., 1982, *Proc. roy. Soc. Lond.*, **A381**, 117.

[3] Field, L., 1996, in *Encyclopedia of NMR*, edited by D. M. Grant and R. K. Harris (Chichester: John Wiley & Sons Ltd), p. 3172.

[4] NANZ, D., ERNST, M., HONG, M., ZIEWGEWEID, M. A., SCHMIDT-ROHR, K., and PINES, A., 1995, *J. magn. Reson.*, **A113,** 169.
[5] SANDSTRÖM, D., and LEVITT, M. H., 1996, *J. Am. chem. Soc.*, **118,** 6966.
[6] COURTIEU, J., BAYLE, J. P., and FUNG, B. M., 1994, *Prog. nucl. magn. Reson. Spectrosc.*, **26,** 141.
[7] JOKISAARI, J., KUONANOJA, J., PULKKINEN, A., and VAANANEN, T., 1981, *Mol. Phys.*, **44,** 197.
[8] M. EDGAR, private communication.
[9] JORGENSEN, W. L., and SEVERANCE, D. L., 1990, *J. Am. chem. Soc.*, **112,** 4768.
[10] DUFFY, E. M., 1990, PhD thesis, Yale University.
[11] RAJNIKANT, and WATKIN, D., 1995, *Acta Cryst.*, **C51,** 1452.
[12] CELEBRE, G., DE LUCA, G., LONGERI, M., SICILIA, E., and EMSLEY, J. W., 1990, *Liq. Cryst.*, **7,** 731.
[13] CELEBRE, G., LONGERI, M., CATALANO, D., VERACINI, C. A., and EMSLEY, J. W., 1991, *J. chem. Soc. Faraday Trans.*, **87,** 2623.
[14] CAMINATI, W., DAMIANI, D., CORBELLI, G., VELINO, B., and BOCK, C. W., 1991, *Mol. Phys.*, **74,** 885.
[15] EMSLEY, J. W., DE LUCA, G., CELEBRE, G., and LONGERI, M., 1996, *Liq. Cryst.*, **20,** 569.
[16] COUNSELL, C. J. R., EMSLEY, J. W., HEATON, N. J., and LUCKHURST, G. R., 1985, *Mol. Phys.*, **54,** 847.
[17] WILSON, M. R., and ALLEN, M. P., 1992, *Liq. Cryst.*, **12,** 157.